Chem

CellPress

Article

Boosting Highly Ordered Porosity in Lanthanum Metal-Organic Frameworks for Ring-Opening Polymerization of γ-Butyrolactone

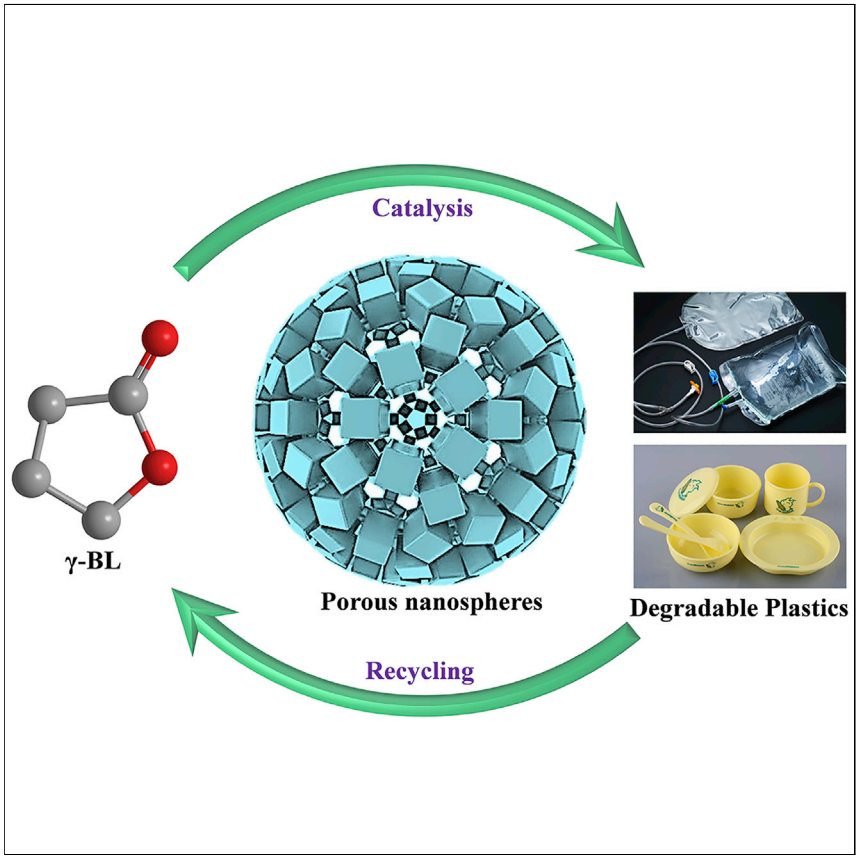

A series of La-MOF-based porous nanospheres have been synthesized through defect engineering and successfully applied as powerful heterogeneous catalysts for ring-opening polymerization of γ-BL with high efficiency and excellent catalyst reusability.

Yifa Chen, Yong-Jun Chen, Yuquan Qi, ..., Yu-He Kan, Shun-Li Li, Ya-Qian Lan

yqlan@njnu.edu.cn

HIGHLIGHTS

A case of heterogeneous catalyst for efficient ring-opening polymerization of γ-BL

The morphology of La-MOF can be tuned into porous nanospheres with tremendous defects

The obtained plastic can be completely recycled by simple heat treatment

Chen et al., Chem 7, 1–17
February 11, 2021
https://doi.org/10.1016/j.chempr.2020.11.019

Please cite this article in press as: Chen et al., Boosting Highly Ordered Porosity in Lanthanum Metal-Organic Frameworks for Ring-Opening Polymerization of γ-Butyrolactone, Chem (2020), https://doi.org/10.1016/j.chempr.2020.11.019

Chem

CellPress

Article

Boosting Highly Ordered Porosity in Lanthanum Metal-Organic Frameworks for Ring-Opening Polymerization of γ-Butyrolactone

Yifa Chen,[1,2,5] Yong-Jun Chen,[1,5] Yuquan Qi,[3,5] Hong-Jing Zhu,[1] Xianqiang Huang,[3] Yi-Rong Wang,[1] Ru-Xin Yang,[1] Yu-He Kan,[4] Shun-Li Li,[1] and Ya-Qian Lan[1,2,6,*]

SUMMARY

γ-butyrolactone (γ-BL), serving as the monomer of biocompatible and recyclable poly(γ-butyrolactone) plastic, faces a giant challenge in ring-opening polymerization (ROP) due to its low strain energy. The ROP of γ-BL is generally achieved under harsh conditions (e.g., high-pressure or gas-protected atmosphere) and is mostly based on homogeneous systems. Here, we synthesize a series of lanthanum metal-organic framework-based porous nanospheres and successfully apply them as heterogeneous catalysts in efficient ROP of γ-BL under mild conditions. Specifically, NNU-mIM-3 presents a yield of 24.6% with low polydispersity distribution centered at 3.6 kDa and the obtained PγBL can be completely and quantitatively recycled into monomers by simple heat treatment. Besides, the ROP catalysis systems have been intensively explored with various imine-based additives, proven to exhibit largely improved performance with PγBL yield of ~50% and Mw of ~8 kDa. This work paves a new way to explore novel heterogeneous catalysts in producing biocompatible and degradable plastics.

INTRODUCTION

Plastics have arisen to be an indispensable part of our daily lives because of their low price, handiness, and functional diversification.[1,2] The broad applications of plastics have conferred great convenience to both industrial applications and human activity, yet, still, coupled with yearly increased environmental problems. In 2018, only about 9% of the total production of plastics (~9.1 billion tons) around the world was recycled and most of it was incinerated, buried, or discard casually in the natural environment.[3] Most plastics with high durability are resistant to biodegradation and can stay in the environment for hundreds of years, causing serious "white pollution" and a global environmental crisis.[4] Therefore, it is of high significance to develop new types of plastics that are biocompatible, degradable, and environmentally friendly.

Aliphatic polyester as a kind of green and renewable polymer material has arisen to be a promising alternative applicable in biomedicine, agriculture and packaging, etc.[5,6] The synthesis methods for aliphatic polyester can be mainly catalyzed into stepwise polycondensation of diols and diacids[7] and ring-opening polymerization (ROP) of the cyclic lactone.[8,9] The former has problems such as high energy consumption (high temperature or vacuum), the poor atomic economy of the polymerization reaction (formation of small molecular by-products such as water), and low molecular weight of the obtained polymer. In contrast, the ROP with the advantages

The Bigger Picture

γ-BL, as a kind of inexpensive and natural renewable compound, is a key downstream chemical of succinic acid that has ranked first in the US Department of Energy's top 12 biomass-derived compounds. However, the ring-opening polymerization (ROP) of γ-BL is mostly limited in homogeneous systems and conducted under harsh conditions (e.g., high-pressure or gas-protected atmosphere, etc.). Here, we report a series of La-MOF-based porous nanospheres and successfully apply them as powerful heterogeneous catalysts for efficient generation of PγBL under normal pressure and air atmosphere. The powerful La-MOF-based nanospheres can efficiently catalyze the ROP of γ-BL with high efficiency, and the obtained PγBL can be completely and quantitatively recycled into monomers by simple heat treatment. During past decades, heterogeneous catalysts have been rarely reported in the ROP of γ-BL. This work provides a starting point for the exploration of porous coordination polymers like MOFs in this area.

Please cite this article in press as: Chen et al., Boosting Highly Ordered Porosity in Lanthanum Metal-Organic Frameworks for Ring-Opening Polymerization of γ-Butyrolactone, Chem (2020), https://doi.org/10.1016/j.chempr.2020.11.019

of low energy consumption, mild conditions, and narrow molecular weight distribution of the product has been intensively investigated for the preparation of aliphatic polyester. Typically, five-membered ring γ-butyrolactone (γ-BL), as a kind of inexpensive and natural renewable compound, is an important precursor for the generation of poly(γ-butyrolactone) (PγBL), a kind of degradable plastic with high biocompatibility.[10–12] Nevertheless, the five-membered ring structure of γ-BL is highly stable and the ring tension (stands for the ring strain contributed by factors such as bond angle distortion, bond stretching or compression or repulsion between eclipsed hydrogen atoms, etc.)[13] is quite weak; therefore, it is hard to provide sufficient negative occurrence by releasing ring tension for successful ROP.[14] Before 2016, only a few studies were reported regarding ROP of γ-BL due to its "unpolymerizable" assertion, and it is only possible to achieve ROP of γ-BL under extreme conditions.[15,16] For example, some work was done on the ROP of γ-BL under severe conditions (160°C, 20,000 atm), but they still resulted in low reaction activity and product molecular weight.[17,18]

The research on the exploration of relatively mild conditions for the ROP of γ-BL has intrigued scientists for decades and is currently undergoing a notable renaissance. To date, some works have reported inspiring results that could realize the reaction under milder conditions and have broken the formidable barrier the ROP of γ-BL, bringing the reaction into relatively easier achieving states. In 2016, the catalyst of $La[N(SiMe_3)_2]_3$ successfully catalyzed the ROP of γ-BL under mild conditions (-40°C, N_2 atmosphere) by controlling thermodynamics and kinetics.[19] This work brings the applicable conditions from the extreme levels into relatively milder ones and, thus, breakes the "unpolymerizable" traditional restraints of γ-BL. After the publication of this breakthrough work, it quickly attracts the attention of the scientific researchers and a series of catalysts (e.g., CTPB [a novel phosphazene superbase], nitrogen-heterocyclic olefins, urea/alkali metal methoxide,^{t}Bu-P_4 [P_4, superbase phosphazene], etc.) have been applied in ROP of γ-BL and its derivatives.[20–27] Despite the progress achieved, these catalysts still have bottlenecks like: (1) the catalyst is sensitive to chemical solvents (e.g., water), and most of them are conducted under anhydrous conditions; (2) most of the catalysis reactions need to be performed under gas-protected atmosphere to eliminate the effect of air; and (3) all of the catalysts reported to date are homogeneous catalysts, which are hard to recycle, and the catalyst residues might affect the properties of the polymer products.[28] Besides, to our knowledge, thus far, there have been no published studies on heterogeneous catalysts for the ROP of γ-BL. Therefore, it is of high importance to explore highly stable heterogeneous catalysts to investigate the ROP of γ-BL under mild conditions.

Metal-organic frameworks (MOFs), a kind of porous crystalline materials constructed from the assembly of metal ions and organic linkers, have attracted broad interest in heterogeneous catalysis due to their superiority in structure tunability, abundant uniformly distributed metal sites, ease of recycling, high porosity, etc.[29–32] In order to achieve highly efficient heterogeneous catalysts suitable for various catalytic environments, the basic properties required for MOF-based catalysts can be mainly concluded as follows: (1) small particle size with accessible porosity to facilitate the mass transfer; (2) unsaturated metal sites with high catalytic activity, and (3) high stability for long-term catalysis reaction.[33,34] In general, well-grown MOF-based crystals through commonly applied methods (e.g., hydrothermal) have relatively large crystal size (commonly in dozens of micrometers) with few defects, which generally lacks in mass transfer efficiency in catalysis. Defect engineering is a promising strategy to transform MOF-based bulk crystals into size-decreased forms, like

[1]Jiangsu Collaborative Innovation Centre of Biomedical Functional Materials, Jiangsu Key Laboratory of New Power Batteries, School of Chemistry and Materials Science, Nanjing Normal University, Nanjing 210023, China

[2]School of Chemistry, South China Normal University, Guangzhou 510006, China

[3]Provincial Key Laboratory of Chemical Energy Storage and Novel Cell Technology, School of Chemistry & Chemical Engineering, Liaocheng University, Liaocheng, Shandong 252059, China

[4]Jiangsu Province Key Laboratory for Chemistry of Low-Dimensional Materials, School of Chemistry and Chemical Engineering, Huaiyin Normal University, Huai'an 223300, China

[5]These authors contributed equally

[6]Lead Contact

*Correspondence: yqlan@njnu.edu.cn

https://doi.org/10.1016/j.chempr.2020.11.019

Please cite this article in press as: Chen et al., Boosting Highly Ordered Porosity in Lanthanum Metal-Organic Frameworks for Ring-Opening Polymerization of γ-Butyrolactone, Chem (2020), https://doi.org/10.1016/j.chempr.2020.11.019

nanoparticles, to create more defects (e.g., exposed metal sites or hierarchical porosity) beneficial for efficient catalysis.[35] We propose to explore La-MOF-based catalysis system through defect engineering and investigate their potential applications in the ROP of γ-BL. Defect engineered La-MOFs, possessing abundant and uniformly distributed La active sites (proven to be effective for the ROP of γ-BL[19]), high porosity, and ease of recycling, might serve as promising heterogeneous catalysts for the ROP of γ-BL under mild conditions. To the best of our knowledge, the exploration of this type of materials has been rarely reported.

Herein, for the first time, we report a series of La-MOF-based highly porous nanospheres through defect engineering and successfully apply them as powerful heterogeneous catalysts for efficient ROP of γ-BL. By regulation with different amounts of 1-methylimidazole (1-mIM), the morphology of La-MOF can be well-tuned from the rod into rod-sphere mixed morphology, then into highly porous nanospheres, and finally into solid nanospheres. Defect engineering can impart La-MOF with tremendous active sites, ultrahigh porosity, and well-tuned morphology, much beneficial for the accessibility of active sites, mass transfer, and improvement of catalysis performance. Specifically, **NNU-mIM-3** presents a yield of 24.6% with low polydispersity distributions (Đ = 1.01) centered at 3.6 kDa and excellent catalyst reusability. The obtained PγBL can be completely and quantitatively recycled into monomers by simply heating the product at 220°C for 1 h. Besides, the reaction system has been intensively explored with various imine-based additives, proven to exhibit largely improved performance with PγBL yield of ~50% and Mw of ~8 kDa. Noteworthy, La-MOF-based nanosphere is the first example of a heterogeneous catalyst applicable in efficient ROP of γ-BL, which provides a starting point for the exploration of MOFs in this area.

RESULTS AND DISCUSSION

Structure and Characterization of La-BTB and NNU-mIM-x (x = 1, 2, 3, 4, and 5)

The synthesis of morphology tuned La-BTB (denoted as **NNU-mIM-x**) is based on the modification of the solvothermal method of La-BTB (Figure 1A). La-BTB is a 3D MOF and possesses a one-dimensional channel with a pore diameter of about 1 nm.[36] La in the structure is trivalent and coordinated with nine oxygen atoms (i.e., two bridging oxygen atoms shared with other adjacent La atoms, the other six oxygen atoms from the carboxyl group of three BTBs, and the last oxygen atom from the solvent molecules that are removable). Generally, **NNU-mIM-x** is synthesized by adding a certain amount of 1-mIM into the solvothermal system of La-BTB (Figure 1A). The motivation of 1-mIM induced defect engineering method aims to transform MOF-based bulk crystals into nanoparticles to create more defects (e.g., exposed metal sites or hierarchical porosity), which might be beneficial for the ROP of γ-BL. Taking **NNU-mIM-3,** for example, 1-mIM (1.2 mL, $V_{1\text{-mIM}}/V_{solvent}$ = 1.5/20) is mixed with $La(NO_3)_3 \cdot 6H_2O$ (0.320 mmol) and 1,3,5-tris(4-carboxyphenyl)benzene (H_3BTB, 0.0816 mmol) in reactor and heated at 85°C. After 24 h, the white powder is collected after centrifugation and washed with N,N-dimethylformamide (DMF) and methanol (MeOH) three times. Powder X-ray diffraction (PXRD) shows that the phase of **NNU-mIM-3** is consistent with simulated La-BTB (Figure 1B). When the amount of 1-mIM is tuned from 0.4 mL (**NNU-mIM-1**, $V_{1\text{-mIM}}/V_{solvent}$ = 0.5/20) to 2.0 mL (**NNU-mIM-5**, $V_{1\text{-mIM}}/V_{solvent}$ = 2.5/20), a series of La-MOFs are synthesized under the same solvothermal conditions and are represented as **NNU-mIM-x** according to the increased amount of 1-mIM (x, stands for the amount of 1-mIM added for every 0.4 mL, for details see Experimental Procedures). PXRD and Fourier-transform infrared spectroscopy

Please cite this article in press as: Chen et al., Boosting Highly Ordered Porosity in Lanthanum Metal-Organic Frameworks for Ring-Opening Polymerization of γ-Butyrolactone, Chem (2020), https://doi.org/10.1016/j.chempr.2020.11.019

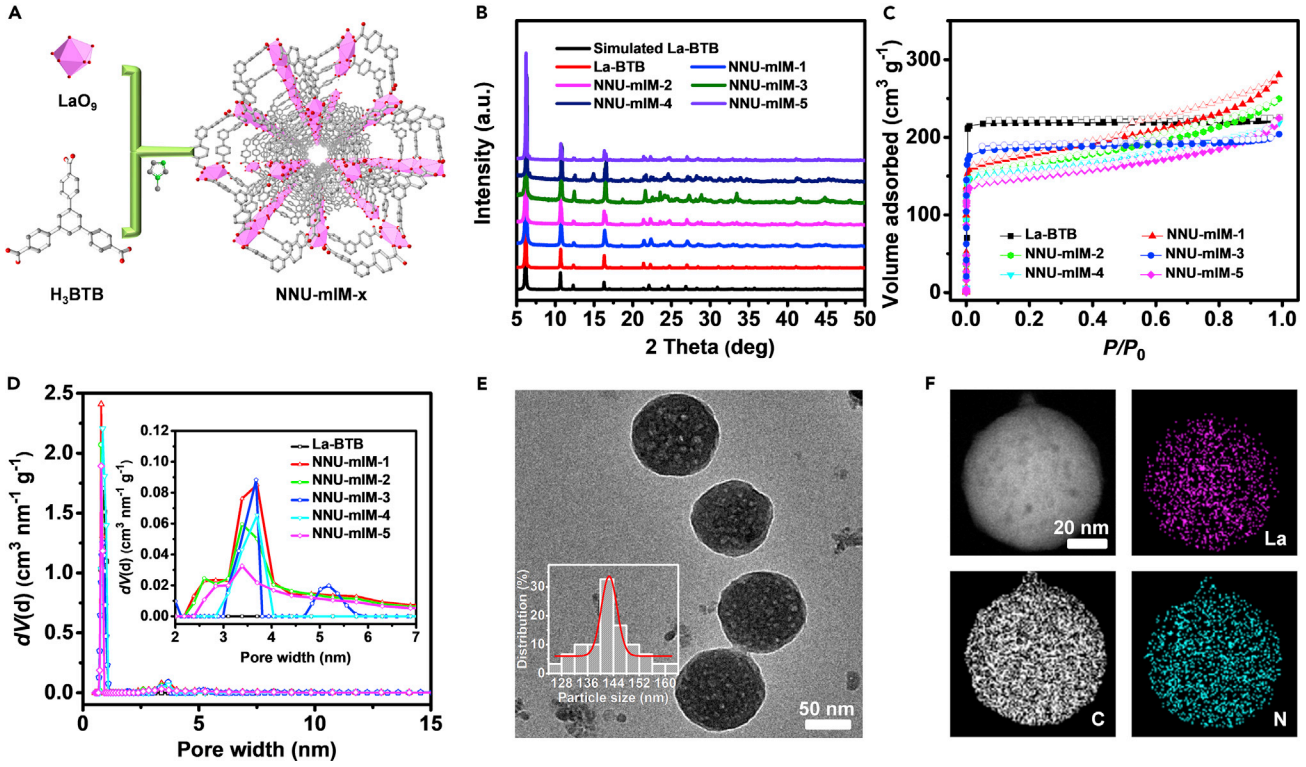

Figure 1. The Structure, Property, and Morphology of La-BTB and NNU-mIM-x (x = 1, 2, 3, 4 and 5)

(A) The structure of **NNU-mIM-x**.

(B) PXRD patterns of La-BTB and **NNU-mIM-x**.

(C) The N_2 sorption curves of La-BTB and **NNU-mIM-x**.

(D) The pore size distribution of La-BTB and **NNU-mIM-x**.

(E) TEM image of **NNU-mIM-3** (inset: the diameter of nanosphere measured by a Nano Measurer software).

(F) The element mapping of **NNU-mIM-3**.

(FT-IR) tests confirm that the internal structures of **NNU-mIM-x** remain intact compared with that of La-BTB (Figures 1B and S1).

To evaluate the porosity of **NNU-mIM-x**, N_2 sorption tests have been conducted. La-BTB exhibits a specific surface area (S_{BET}) of 823 $m^2\ g^{-1}$ and pore size distribution fitted at 0.97 nm, which matches well with the structure of La-BTB (Figures 1C and 1D).[36] After the addition of 1-mIM, the S_{BET} and pore volume (V_t) of **NNU-mIM-x** slightly decrease, possibly attributed to the generation of defects. For example, the S_{BET} and V_t of **NNU-mIM-3** are 564 $m^2\ g^{-1}$ and 0.504 $cm^3\ g^{-1}$, respectively, which are slightly lower than that of La-BTB (S_{BET}, 823 $m^2\ g^{-1}$ and V_t, 0.609 $cm^3\ g^{-1}$). After regulation with different amounts of 1-mIM, the pore size distribution of **NNU-mIM-x** extends from micro-pore to meso/macro-pore range (Figure 1D). With the enhancement of 1-mIM amount, the micro-pore volume slightly decreases (V_{micro}: La-BTB, 0.595 $cm^3\ g^{-1}$; **NNU-mIM-3**, 0.412 $cm^3\ g^{-1}$ and **NNU-mIM-5**, 0.243 $cm^3\ g^{-1}$) coupling with the largely increased meso/macro-pore volume ($V_{meso/macro}$: La-BTB, 0.001 $cm^3\ g^{-1}$; **NNU-mIM-3**, 0.092 $cm^3\ g^{-1}$ and **NNU-mIM-5**, 0.112 $cm^3\ g^{-1}$) (Figure 1D; Table S1). The meso/macro-pore volumes of **NNU-mIM-3** and **NNU-mIM-5** are almost 90 and 110 times higher than that of La-BTB. Therefore, the 1-mIM induceddefect engineering method successfully extends the porosity of La-BTB from the micro-pore region to the meso/macro-pore region, which might be beneficial for the mass transfer and the expose of La active sites to facilitate the ROP of γ-BL.

Please cite this article in press as: Chen et al., Boosting Highly Ordered Porosity in Lanthanum Metal-Organic Frameworks for Ring-Opening Polymerization of γ-Butyrolactone, Chem (2020), https://doi.org/10.1016/j.chempr.2020.11.019

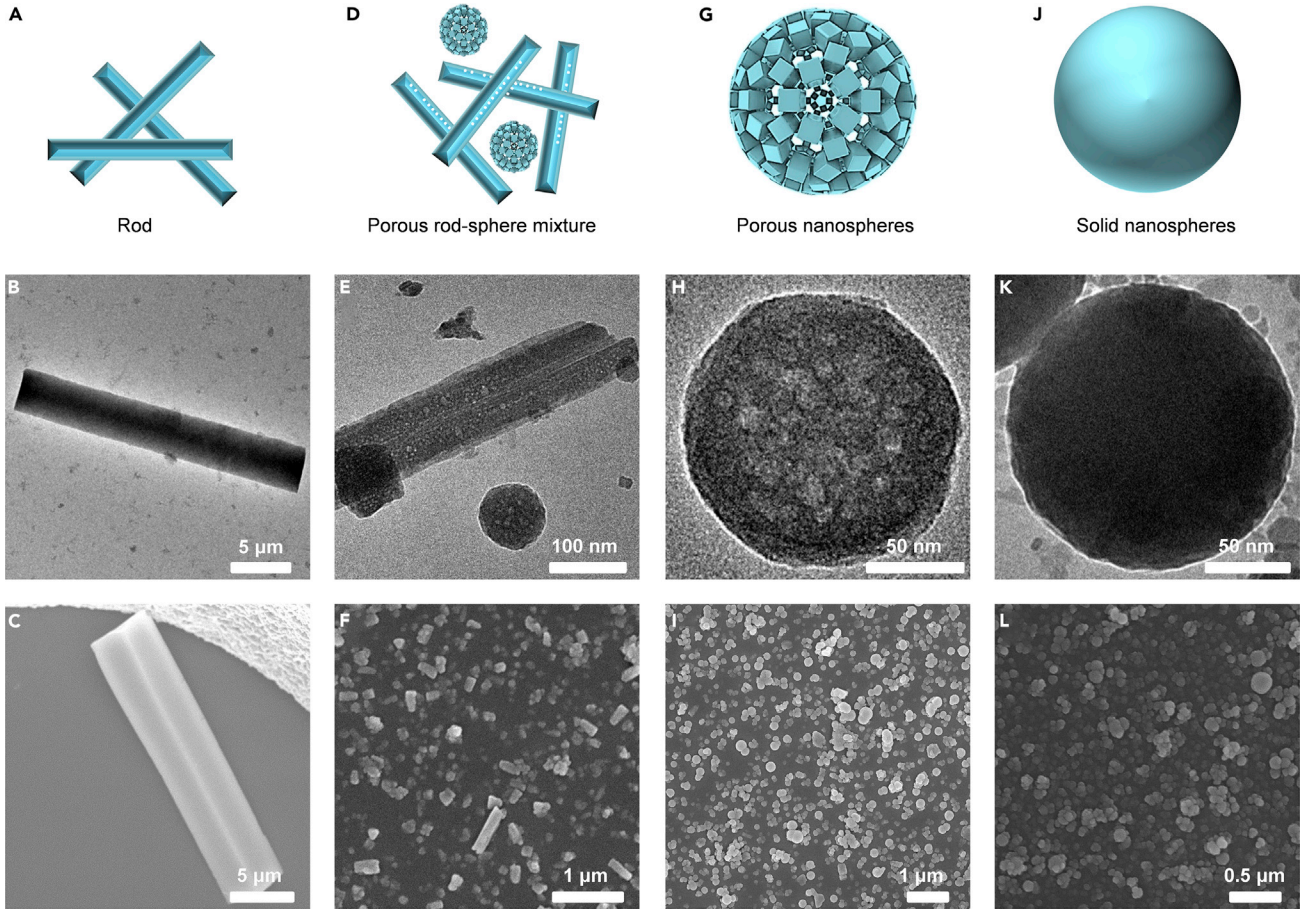

Figure 2. The Tuning of NNU-mIM-x Morphology with Diverse Volume Ratios of 1-mIM to Solvent ($V_{1\text{-mIM}}/V_{solvent}$)

(A–C) La-BTB ($V_{1\text{-mIM}}/V_{solvent}$ = 0, La-BTB is equivalent to **NNU-mIM-0**): (A) Schematic diagram, (B) TEM image, (C) SEM image.

(D–F) **NNU-mIM**-2 ($V_{1\text{-mIM}}/V_{solvent}$ = 1/20).

(G–I) **NNU-mIM**-3 ($V_{1\text{-mIM}}/V_{solvent}$ = 1.5/20).

(J–L) **NNU-mIM**-7 ($V_{1\text{-mIM}}/V_{solvent}$ = 3.5/20).

The existence of large amount meso/macro-pores in **NNU-mIM-x** might be attributed to the generation of numerous defects in the structure. To further prove it and study the defects, scanning electron microscopy (SEM) and transmission electron microscopy (TEM) tests were conducted. La-BTB is a rod-like morphology (length, ~3.4 μm, and width, ~0.5 μm) with uniformly distributed elements as proved by SEM, TEM, and element mapping characterizations (Figures 2A–2C and S2). With the addition of 1-mIM, the morphology of La-BTB changes accordingly. When small amount of 1-mIM is added ($V_{1\text{-mIM}}/V_{solvent}$ = 1/20), **NNU-mIM-2** presents rod-sphere mixture morphology (Figure 2D). Interestingly, there is large amount of vacancy detected in the rod-sphere mixed morphology proved by SEM and TEM tests, possibly due to the addition of 1-mIM that can create defects during the formation process (Figures 2E and 2F). Furthermore, when the amount of 1-mIM is among the range of $V_{1\text{-mIM}}/V_{solvent}$ = (1.5-3)/20, the morphology of the material completely transforms into porous nanospheres (Figures 2G–2I and S3). For example, **NNU-mIM-3** ($V_{1\text{-mIM}}/V_{solvent}$ = 1.5/20) displays a kind of nanosphere morphology with a diameter of about 142 nm and spherical vacancies with diameter about 9.2 nm proved by SEM and TEM tests (Figures 1E and S3A–S3C). The corresponding element mappings of **NNU-mIM-3** show that elements (La, C, and N) are uniformly distributed in the sample

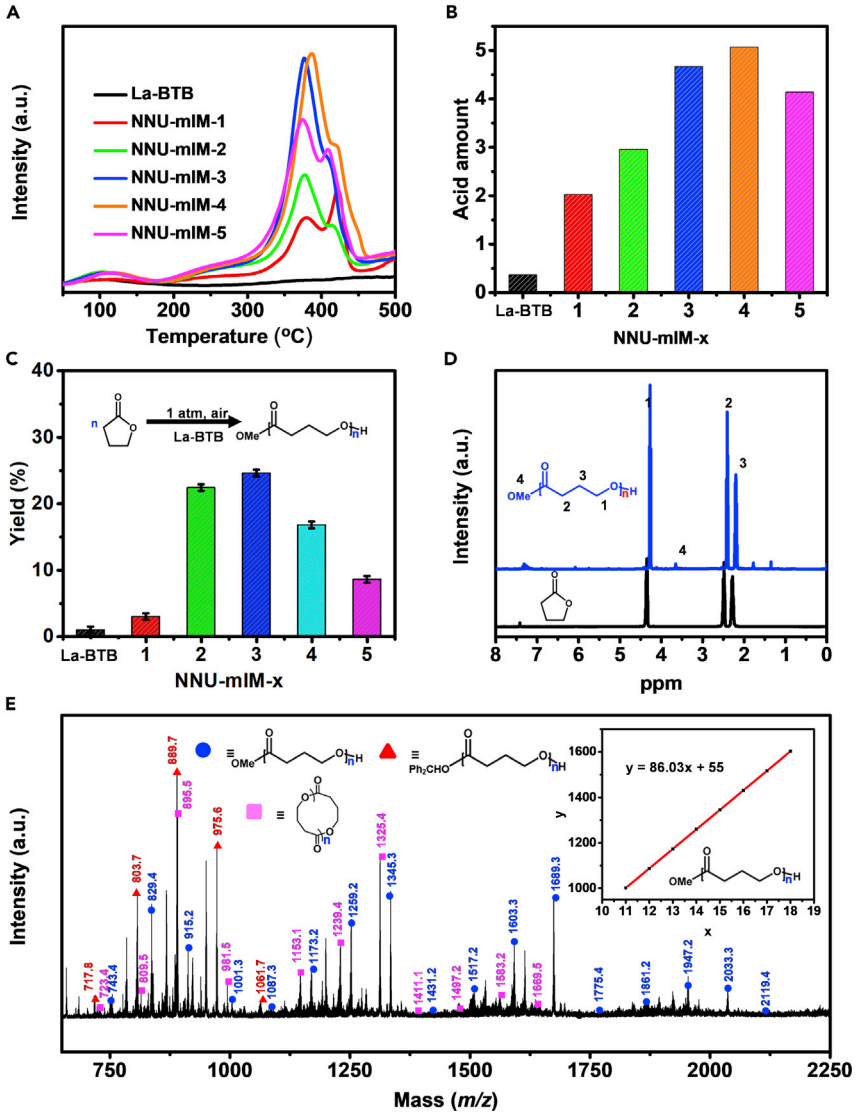

Figure 3. The NH_3-TPD Results and Catalysis Performance of La-BTB and NNU-mIM-x (x = 1, 2, 3, 4, and 5)

(A) NH_3-TPD results of La-BTB and **NNU-mIM-x**.

(B) The acid amount of La-BTB and **NNU-mIM-x** calculated based on peak area (> 200°C) (La-BTB is equivalent to **NNU-mIM-0**).

(C) Catalysis performance of La-BTB and **NNU-mIM-x**.

(D) ^1H NMR spectra ($CDCl_3$, δ 7.26 ppm, 25°C) of obtained PγBL and γ-BL.

(E) MALDI-TOF mass spectra of PγBL (inset: plot of *m/z* values [y] versus the number of γ-BL repeat units [x]).

(Figure 1F). The numerous La metal sites coupling with a large amount of defects in the nanospheres might provide tremendous accessible active sites for the efficient ROP of γ-BL. Besides, the diameters of spherical vacancies for **NNU-mIM-x**-based porous nanospheres have been calculated. For **NNU-mIM-4**, the average diameter of spherical vacancies is calculated to be ~11.6 nm, which is higher than that of **NNU-mIM-3** (~9.2 nm, Figures 3D–3F). After that, the diameter of spherical vacancies decreases with the increased addition of 1-mIM (**NNU-mIM-5**, ~9.6 nm and **NNU-mIM-6**, ~6.5 nm) and the spherical vacancies completely disappear from the range **NNU-mIM-7** ($V_{1\text{-mIM}}/V_{solvent}$ = 3.5/20) to **NNU-mIM-9**

Please cite this article in press as: Chen et al., Boosting Highly Ordered Porosity in Lanthanum Metal-Organic Frameworks for Ring-Opening Polymerization of γ-Butyrolactone, Chem (2020), https://doi.org/10.1016/j.chempr.2020.11.019

($V_{1\text{-mIM}}/V_{solvent}$ = 4.5/20) (Figures S3–S5). Above all, the morphology regulation of La-BTB with different amounts of 1-mIM ($V_{1\text{-mIM}}/V_{solvent}$, (0–4.5)/20) can endow the morphology change among rod shape, porous rod-sphere mixture, well-tuned porous and solid nanospheres (Figures 2 and S3–S5). However, if larger amount of 1-mIM ($V_{1\text{-mIM}}/V_{solvent}$, > 4.5/20) is added, the inert structure of La-BTB cannot be remained, which would be attributed to the excessive addition of 1-mIM and might disrupt the formation process of La-BTB (Figure S6).

It is noteworthy that **NNU-mIM-x** exhibits high chemical and thermal stability. To test the chemical stability, the sample is immersed in a series of solvents for several days and measured by PXRD characterization. Taking **NNU-mIM-3**, for example, the structural integrity of **NNU-mIM-3** remains unchanged after immersing in common organic solvents (e.g., aniline, tetrahydrofuran, and chloroform, etc.) for 3 days compared with as-synthesized one (Figure S7). In addition, **NNU-mIM-3** can be stable in water (>10 days) and even in boiling water (100°C, >3 days) (Figure S7). Moreover, **NNU-mIM-3** is tolerant of harsh acidic or basic conditions with a wide pH range from 1 to 12 (Figure S7). For thermal stability, the inherent structure of **NNU-mIM-3** remains intact both under 500°C (N_2 atmosphere) and 400°C (air atmosphere), as certified by variable temperature PXRD tests (Figure S8).

To further reveal the valance states of **NNU-mIM-x**, X-ray photoelectron spectroscopy (XPS) tests were conducted. Lanthanum in the structures of La-BTB and **NNU-mIM-x** is trivalent as shown by XPS tests (Figure S9). Taking **NNU-mIM-3**, for example, a new weak peak of **NNU-mIM-3** appears at 856.6 eV compared with that of La-BTB, which might be ascribed to the peak position of La-N at 856.4 eV (Figure S9B).[37] This indicates that the addition of 1-mIM might substitute the solvent molecule like water. Further, proven by the elemental and inductive coupled plasma emission spectrometer (ICP) analyses, the formula of **NNU-mIM-3** is calculated to be $La(BTB)_{0.63}(DMF)_{0.19}(1\text{-mIM})_{0.13}(H_2O)_{0.8}$. Relative formulas of **NNU-mIM-x** are presented in Table S2.

As mentioned above, a large amount of defects have been created in the highly porous and stable samples. To evaluate the amount of defects, NH_3 temperature-programmed desorption (NH_3-TPD) tests are performed to accurately determine the defects in **NNU-mIM-x**. The NH_3-TPD peak at about 100°C reflects the physical sorption of NH_3 and peaks higher than 200°C are attributed to different acid sites like Lewis acid sites (e.g., unsaturated metal sites) or Brønsted acid sites (e.g., uncoordinated carboxyl groups).[38,39] The peak intensity both for physical and acid site sorption of **NNU-mIM-x** in these curves are stronger than La-BTB (Figure 3A). Especially, the physical sorption amount of **NNU-mIM-x** are calculated to be 0.022, 0.046, 0.046, 0.041, and 0.039 mmol g^{-1}, respectively, which is much higher than that of La-BTB (0.018 mmol g^{-1}) (Figure 3A). Besides, the acid site amount of **NNU-mIM-x** are calculated to be 2.03, 2.96, 4.67, 5.07, and 4.14 mmol g^{-1} based on the integral area of NH_3-TPD curves, respectively (Figure 3B). The acid site amount of **NNU-mIM-3** and **NNU-mIM-4** are about 12 and 14 times larger than that of La-BTB (0.37 mmol g^{-1}), which suggests that **NNU-mIM-3** and **NNU-mIM-4** expose more defects like Lewis acid and Brønsted acid sites.[40,41] Further certified by the molecular formulas of **NNU-mIM-x**, the amount of BTB and H_2O molecules in **NNU-mIM-x** were slightly decreased based on the elemental and ICP analyses, which indicates that more surface defects and active sites were exposed with the increased addition of 1-mIM (Table S2). The results were also confirmed by thermogravimetric analyses (TGA) results (tested under air atmosphere), in which the ratio of La/BTB were detected and analyzed (Figure S10). Especially, the formula results of **NNU-mIM-x**

Please cite this article in press as: Chen et al., Boosting Highly Ordered Porosity in Lanthanum Metal-Organic Frameworks for Ring-Opening Polymerization of γ-Butyrolactone, Chem (2020), https://doi.org/10.1016/j.chempr.2020.11.019

match well with the elemental and ICP tests. Therefore, **NNU-mIM-x** all possess more exposed defects and active sites than La-BTB through the regulation of 1-mIM, which might dramatically improve their catalytic activity.

The Catalytic Performance of La-BTB and NNU-mIM-x (x = 1, 2, 3, 4, and 5)

With the regulation of 1-mIM, **NNU-mIM-x** presents highly porous morphology, high chemical or thermal stability, and exposes numerous active sites compared with La-BTB. With this in mind, we intend to explore the catalytic performance of La-BTB and **NNU-mIM-x** in the ROP of γ-BL. The ROP of γ-BL is highly important to generate PγBL, a powerful plastic product with high biocompatibility and excellent recyclability that can be completely degraded into monomers at suitable temperatures (200°C–300°C).[13,42] As the first case of heterogeneous catalysts to explore their performance in ROP of γ-BL, it might broaden the application range of MOF catalysts and open up new ideas for the polymerization of γ-BL.

As a proof-of-concept, the catalytic performance of **NNU-mIM-x** for the ROP of γ-BL are tested at −40°C, air condition, and 24 h. The yields of PγBL display a volcano-shape curve for **NNU-mIM-x** and the trend is similar to the defect results detected in the NH_3-TPD tests (Figures 3B and 3C). It dramatically increases for **NNU-mIM-2** (22.4%) possessing a large amount of spherical vacancies in the rod-sphere mixture morphology, which is superior to that of **NNU-mIM-1** (3.0%) with solid rod-like morphology (Figures 3C, S4A, and S4D). The yield reaches up to a maximum value of 24.6% for **NNU-mIM-3** with porous nanosphere morphology (Figures 2G–2I). After that, the yields decrease to 16.8% for **NNU-mIM-4** and 8.6% for **NNU-mIM-5**, respectively (Figure 3C). Noteworthy, all of **NNU-mIM-x** exhibit higher performance than that of La-BTB (1.0%), complying with the defect results detected in NH_3-TPD tests (Figure 3B). This result implies the vital role of defects that would largely increase the catalytic performance of **NNU-mIM-x**. Moreover, the proprieties of **NNU-mIM-x** presented match well with the results as verified by the NH_3-TPD (Figure 3B) and morphology tests (Figures 2 and S3–S5). The achieved performance indicates that the amount of defect is closely related to the catalytic performance and the higher in defect amount, the better performance achieved, which might possibly due to the generated defect is beneficial for the accessibility of active sites, mass transfer, and improvement of catalysis performance.

Based on the above results, **NNU-mIM-3** with the best catalytic performance is selected to explore the kinetic study. In the kinetic study, we find that the performance of **NNU-mIM-3** is increased from 6 to 24 h and the best performance is achieved with 24 h (i.e., 6 h, 3.2%; 12 h, 11.6%; 18 h, 17.5% and 24 h, 24.6%) (Figure S11A). When the reaction time is longer than 24 h, the polymer yield remains almost unchanged, implying the termination of reaction at ~24 h (Figure S11A). Therefore, the result suggests 24 h to be the best reaction time in the kinetic study. Moreover, different temperatures ranging from 0°C to −40°C have been evaluated to determine the best reaction temperature (Figure S11B). With the increase of temperature, the poorer performance has been achieved, implying -40°C to be the best one for the ROP of γ-BL. These results are in accordance with the reported homogeneous catalysis systems.[19,21] Besides, the superiority of **NNU-mIM-x** in catalysis is further supported by the contrast experiments, in which H_3BTB and $La(NO_3)_3 \cdot 6H_2O$ exhibit almost no catalytic activity for the ROP of γ-BL (details see Experimental Procedures).

To characterize the obtained product, nuclear magnetic resonance spectroscopy (^1H NMR), matrix-assisted laser desorption/ionization time-of-flight mass spectroscopy

Please cite this article in press as: Chen et al., Boosting Highly Ordered Porosity in Lanthanum Metal-Organic Frameworks for Ring-Opening Polymerization of γ-Butyrolactone, Chem (2020), https://doi.org/10.1016/j.chempr.2020.11.019

(MALDI-TOF MS) and gel-permeation chromatography (GPC) are performed. Taking the product obtained from the catalysis reaction by **NNU-mIM-3** for example, apparent chemical shift (~0.1 ppm) is detected in ^{1}H NMR spectrum when compared the product with that of γ-BL (Figure 3D). Aside from the major signals at δ 4.2, 2.4 and 2.1 ppm that are ascribed to the protons of the main chain (-[C(=O)$CH_2CH_2CH_2O]_n^-$), minor signals attributed to the chain-end groups (MeO/H) have also been detected, which implies the successful conversion of γ-BL into PγBL and confirms the possible coordination-insertion mechanism of La-based complex as reported in the literature (Figure 3D).[19–21] MALDI-TOF MS is further conducted to analyze the component of the product. From the MALDI-TOF MS spectrum, the data spacing among the three neighboring molecular ion peaks within each series is the exact molar mass of the repeat unit, γ-BL (m/z = 86.03), as shown by the slopes of the linear plots of m/z values (y) vs the number of γ-BL repeat units (x) (Figure 3E). According to the results observed from the MALDI-TOF MS, the intercepts of the plots indicate there are three kinds of polymers obtained: the cyclic PγBL with no chain ends [M_{end} = 0 + 23 (Na^+) g/mol], denoted as $[\gamma\text{-BL}]_n$; the linear PγBL with MeO/H as chain ends [M_{end} = 32 (MeO/H) + 23 (Na^+) g/mol], denoted as MeO-$[\gamma\text{-BL}]_n$-H and the linear PγBL with Ph_2CHO/H as chain ends [M_{end} = 184.3 (Ph_2CHO/H) + 23 (Na^+) g/mol], denoted as Ph_2CHO-$[\gamma\text{-BL}]_n$-H (Figures 3E and S12). As revealed in the spectrum, PγBL produced is predominantly linear MeO-$[\gamma\text{-BL}]_n$-H (y = 86.03x + 55), minor liner Ph_2CHO-$[\gamma\text{-BL}]_n$-H (y = 86.03x + 207.2) and cyclic $[\gamma\text{-BL}]_n$ (y = 86.03x + 23) component (Figures 3E and S12). Base on the characterization of the obtained PγBL, we found that it can control the cyclic *vs* linear synthesis in the generation of PγBL. When the catalysts are La-BTB or **NNU-mIM-x** (x = 1, 2 and 3) ($V_{1\text{-mIM}}/V_{solvent}$ = (0–1.5)/20), the components of PγBL produced are predominantly linear MeO-$[\gamma\text{-BL}]_n$-H (y = 86.03x + 55) and Ph_2CHO-$[\gamma\text{-BL}]_n$-H (y = 86.03x + 207.2) (Figures S12 and S19). While if the catalysts are **NNU-mIM-4** and **NNU-mIM-5** ($V_{1\text{-mIM}}/V_{solvent}$ = (2-2.5)/20), the components of PγBL produced are predominantly cyclic $[\gamma\text{-BL}]_n$ (y = 86.03x + 23) (Figures S12 and S19). Specifically, the production of PγBL structure is mostly in line with the trend that the linear PγBL is gradually decreased coupling with the increase of cyclic PγBL when the catalysts change from La-BTB to **NNU-mIM-5** (Figure S19). The result might be attributed to the varied properties like porosity (e.g., pore size or pore volume, etc.), exposed active sites, or morphology in these catalysts that would provide diverse activity or steric effects for the selective production of PγBL with a cyclic or linear structure. Moreover, GPC tests with light scattering, refractive index, and viscosity triple detection have been applied to analyze the obtained PγBL materials. Specifically, PγBL shows a number-average molecular weight (M_n) of 3.6 kDa and a polydispersity index (Đ = M_w/M_n, M_w stands for weight-average molecular weight) of 1.01 (Figure S13). In addition, this reaction is conducted under mild conditions (e.g., normal pressure and air atmosphere), surpassing the reported homogeneous catalysts in which the conditions are generally sensitive to chemical solvents (e.g., water) and the catalysis reactions need to be conducted under a gas-protected atmosphere or high-pressure conditions.[17–27]

Recyclability is an important parameter to study the durability of the catalysts.[43,44] **NNU-mIM-3** with the best catalytic performance is selected to investigate the recycle experiment. After catalysis, the recovered **NNU-mIM-3** can be reused in repetitive reactions with negligible loss of its high catalytic performance for five cycles [yields, 24.6% (first run), 23.8% (second run), 25.1% (third run), 23.4% (forth run) and 23.7% (fifth run)] (Figure 4A). The structural integrity of **NNU-mIM-3** remains intact after five catalysis cycles as proved by the PXRD tests (Figure 4B). The N_2 sorption test is carried out to evaluate the porosity of **NNU-mIM-3** after catalysis. A slightly

Please cite this article in press as: Chen et al., Boosting Highly Ordered Porosity in Lanthanum Metal-Organic Frameworks for Ring-Opening Polymerization of γ-Butyrolactone, Chem (2020), https://doi.org/10.1016/j.chempr.2020.11.019

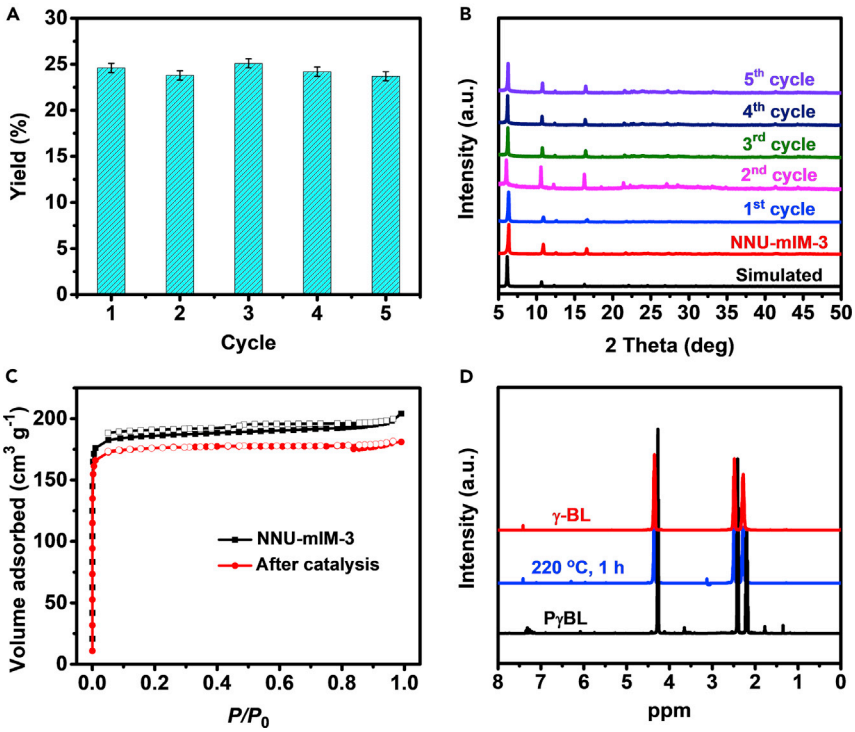

Figure 4. The Recyclability Tests of NNU-mIM-3 and Thermal Feedstock Recycling of PγBL

(A) The recycling performance of **NNU-mIM-3**.

(B) The PXRD patterns of **NNU-mIM-3** in recycle experiments.

(C) The N_2 sorption curves of **NNU-mIM-3** before and after catalysis experiments.

(D) ^{1}H NMR spectra of pristine γ-BL, PγBL and PγBL after heat treatment (220°C, 1 h).

decreased S_{BET} (523 $m^2\ g^{-1}$) and similar pore size distribution are detected when compared with that of **NNU-mIM-3** (S_{BET}, 564 $m^2\ g^{-1}$) (Figures 4C and S14). Besides, the morphology of **NNU-mIM-3** after the catalytic experiment is revealed by TEM test and the maintained porous nanosphere morphology with numerous spherical vacancies supports the integrity of **NNU-mIM-3** after catalysis (Figure S15). Furthermore, the FT-IR of the **NNU-mIM-3** recovered after catalytic experiments are consistent with the as-prepared sample, which suggests the remained underlying topology of **NNU-mIM-3** (Figure S16B). Moreover, a negligible leaching element of La is detected (< 0.02 mg L^{-1}) in the product, which further verifies the high durability of the material. For homogeneous catalysts, the remained catalyst residues in the products might have a negative effect on the properties of polymer products and they still face the problems like hard in recycling. In this work, heterogeneous catalysts like **NNU-mIM-3** are ease of recycling and can get rid of these problems. To prove it, the FT-IR and PXRD tests of the product polymer show that the catalyst is successfully and completely separated from the product after recycling (Figure S16). In order to prove the easy degradation of the PγBL, the thermal recyclability test of PγBL product is investigated through a heat treating experiment. After heating the product at 220°C for 1 hour in a stainless-steel reactor, colorless liquid is directly (without any purification) obtained after cooling to room temperature. The colorless liquid is further analyzed by ^{1}H NMR spectroscopy and the peaks match well with that of γ-BL, indicating the complete conversion of PγBL into γ-BL after thermal treatment (Figure 4D).

Besides, we have conducted the catalytic experiments of NNU-mIM-3 for the ROP of other lactones to investigate the versatility of these materials, including

Please cite this article in press as: Chen et al., Boosting Highly Ordered Porosity in Lanthanum Metal-Organic Frameworks for Ring-Opening Polymerization of γ-Butyrolactone, Chem (2020), https://doi.org/10.1016/j.chempr.2020.11.019

β-butyrolactone (β-BL) or δ-valerolactone (δ-VL) (Figure S18A).[45,46] To evaluate the performance of **NNU-mIM-3** for the ROP of these lactones, we firstly investigate the performance under similar experimental conditions as that of γ-BL. We find that almost no polymers are produced at temperatures ranging from −40°C to −10°C. Surprisingly, **NNU-mIM-3** exhibits polymer yields of 15.8% and 26.8% for β-BL and δ-VL at room temperature, respectively (Figure S18). These might be attributed to the different reaction activity of β-BL and δ-VL in the ROP reaction when compared with that of γ-BL.

The Exploration of Catalytic Performance with Various Imine-Based Additives

Based on the above results, it seems to have monomer-polymer thermodynamic equilibrium for the ROP reaction owing to their relatively low polymer yield (24.6%) and average molecular weight (~3.6 kDa). To disrupt the thermodynamic equilibrium, various additives have been applied to further improve the performance. Interesting results have been obtained through adding various additives (e.g., diethylamine, triethylamine, 1-methylimidazole, 1,10-phenanthroli, 5-bromosalicylic, and benzenesulfonic acid, etc.) and adjusting the amounts of them (Table S3). Among all of the additives, we find that the polymer yields have been largely improved by adding diethylamine, while other additives like acid or alkaline additives have unchanged or even negative effect on the performance (Table S3). To determine the influence of the diethylamine, different amounts of diethylamine (i.e., 0 to 30 μL) have been tested to optimize the best performance (Figure S17). When the amounts of diethylamine are increased from 0 to 20 μL, the polymer yields are correspondingly increased (i.e., 0 μL, 24.6%; 10 μL, 26.2% and 20 μL, 38.4%). However, the yield (34.2%) starts to decrease with the diethylamine amount of 30 μL (Figure S17). After carefully adjusting the amount of diethylamine, the optimized yield can be largely increased from 24.6% to 38.4%. With the superior performance of diethylamine over other acid or alkaline additives in hand, we suppose that diethylamine as a kind of imine-based additives with basicity (pK_a, ~11.02) and coordination ability, might serve as the role of CTPB[21] to generate intermediate with Ph_2CHOH or coordination agent with La active sites in La-BTB (similar as La $[N(SiMe_3)_2]_3$)[19] to facilitate the ROP of γ-BL and improve the catalysis properties.

In this regard, we further extend the system to other imine-based additives. Aside from the diethylamine, we have further conducted numerous experiments based on another twelve kinds of imine-based additives and adjusted the amounts of them to optimize the best performance (Figure 5C). These imine-based additives, such as N-ethylbenzylamine, diisopropylamine, N-ethylpropan-1-amine, and 3-fluoro-N-methylbenzylamine, possessing basic properties with pK_a values range from 9.39 to 11.07, have been selected to explore the catalysis performance. Taking diisopropylamine as an example, the polymer yield follows a volcano-shape trend in tuning the different amounts of additives, and the highest polymer yield achieved at 48.2% with the addition of 20 μL (Figure 5A). When the amount of diisopropylamine largely increases to a similar mole amount of γ-BL, the polymer yield slightly decreases to 41.9% (Table S4). Therefore, 20 μL and a similar mole amount of γ-BL were selected as two examples to investigate the influence of additives on the catalysis properties. Among all of the imine-based additives, we found that all of them have improved the polymer yields to some extent when compared with the reaction without additive (24.6%) (Figure 5C; Table S4). In detail, the addition of 20 μL N-methylbenzylamine, N-ethylbenzylamine, N-(tert-Butyl)benzylamine, N-isopropylbenzylamine and 3-fluoro-N-methylbenzylamine, a group of phenyl and imine-based additives, present polymer yields of 32.2% to 43.1% (Figure 5C; Table S4, entry 1–5). The polymer yields are mostly increased when the additive amount is

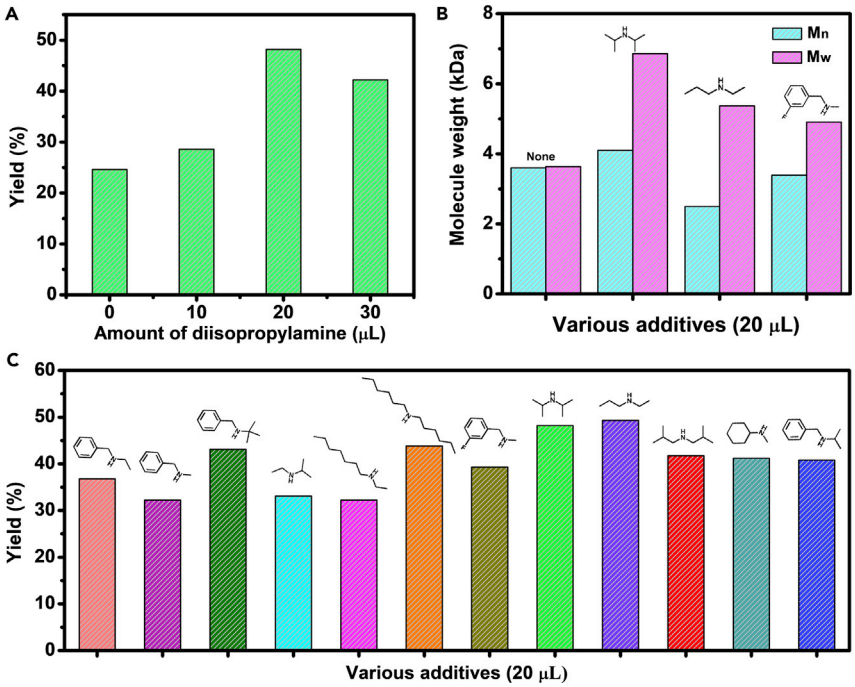

Figure 5. The Catalysis Performance of NNU-mIM-3 with the Addition of Various Imine-Based Additives

(A) The catalysis performance of **NNU-mIM-3** with the addition of diisopropylamine.

(B) The average molecular weight of the products with the addition of 20 μL diisopropylamine, N-ethylpropan-1-amine, and 3-fluoro-N-methylbenzylamine.

(C) The polymer yields of **NNU-mIM-3** with the addition of various imine-based additives.

The recycle performance of **NNU-mIM-3**.

the same mole amount of γ-BL and the best of them, 3-fluoro-N-methylbenzylamine shows superior yield (50.2%) over others, which might be attributed to existence of functional groups like fluorine or methyl group that would tune the coordination ability of these compounds to possess diverse effects on the ROP reactions (Table S4, entry 1–5). Interestingly, another group of additives, such as diisopropylamine, N-ethylpropan-1-amine, dihexylamine, diisobutylamine, and N-methylcyclohexylamine show distinct performance and the yields with 20 μL additive are larger than that of the same mole amount of γ-BL (Table S4, entry 6–10). The distinct phenomenon might be ascribed to the higher pK_a than the first group that the stronger basicity would lead to poorer yield when an excessive amount of additives are added (Table S4).

Specifically, the pristine polymer yield (24.6%) can be largely improved to 48.2%, 49.3%, and 50.2% with the addition of diisopropylamine, N-ethylpropan-1-amine, and 3-fluoro-N-methylbenzylamine respectively (Figure 5C). In this regard, diisopropylamine, N-ethylpropan-1-amine, and 3-fluoro-N-methylbenzylamine with the best performance are picked as three examples to investigate the properties of products. To get rid of the possibility of imine-based additives as the catalysts by themselves, contrast ROP reactions that without **NNU-mIM-3** have been conducted and no products are detected under similar conditions, indicating them to be a kind of co-catalyst that cooperates with **NNU-mIM-3** to facilitate the ROP reaction. In addition, GPC tests have been performed to evaluate the average molecular weight (Figures S20 and S21). With the addition of 20 μL diisopropylamine, the GPC results show that

the Mn and Mw of the product increase from ~3.6 kDa to 4.1 kDa and 6.8 kDa, respectively (Table S5, entry 2). If the amount of diisopropylamine enhances to the similar mole amount of γ-BL, the Mw (8.3 kDa) has been largely increased while the Mn (3.4 kDa) remains almost unchanged (Figure S21). Similarly, N-ethylpropan-1-amine and 3-fluoro-N-methylbenzylamine display approximately trend with largely increased Mw when the additive amount increases from 20 μL to the similar mole amount of γ-BL (Table S5, entry 3). Noteworthy, the Mn and Mw can be largely improved to 4.8 kDa and 8.4 kDa for the addition of 3-fluoro-N-methylbenzylamine with a similar mole amount of γ-BL, respectively (Table S5, entry 3). Therefore, the imine-based additives have a positive effect on the improvement of both polymer yield and average molecular weight for the ROP of γ-BL. Besides, the recycling experiments with the addition of 20 μL diisopropylamine show that **NNU-mIM-3** can be recycled for three times with slight decrease in polymer yield and retained structure integrity (Figure S22). The polymer yields of reported homogeneous catalysts are mostly below 40%[23,27] and only some examples are higher than 60%.[18] The optimized results (yield, ~50% and Mw, ~8 kDa) in our work are comparable to most of reported homogeneous catalysts.[17–27]

Conclusions

In summary, we report a defect engineering method to explore a series of newly designed La-MOF-based heterogeneous catalysts for efficient ROP of γ-BL. Regulation by different amounts of 1-mIM, the morphology of La-MOF changes from the rod-like shape into rod-sphere mixed morphology, and finally into specially designed porous nanosphere morphology. Defect engineering imparts these materials with tremendous active sites, ultrahigh porosity, and a large amount of defects that can be successfully applied in efficient ROP of γ-BL. Specifically, NNU-mIM-3 presents a yield of 24.6% with low polydispersity distributions (Đ = 1.01) centered at 3.6 kDa and excellent catalyst reusability. The obtained PγBL can be quantitatively recycled into monomers by simple heat treatment and the catalyst can be well-recycled with accessible pores and maintained structures. In addition, we have further extended the catalysis system to other lactones and investigated the effect of various imine-based additives to largely improve the performance (yield, ~50% and Mw, ~8 kDa). The performance achieved can be comparable to most of the homogeneous catalysts. This general strategy, accompanied by the exploration of new La-MOFs with high stability, would herald an era in promoting the application range of MOF-based heterogeneous catalysts in the ROP ofγ-BL.

EXPERIMENTAL PROCEDURES

Resource Availability

Lead Contact

Further information and requests for resources should be directed to and will be fulfilled by the Lead Contact, Ya-Qian Lan (yqlan@njnu.edu.cn).

Materials Availability

This study did not generate new unique reagents.

Data and Code Availability

The published article includes all datasets generated during this study.

Synthesis of La-BTB

The synthesis of La-BTB follows the procedures reported in the literature.[36] $La(NO_3)_3 \cdot 6H_2O$ (138.6 mg, 0.320 mmol) were dissolved in 16 mL DMF/MeOH/H_2O (6:6:1) mixed solution with ultrasound for about 5 min in a 20 mL flask. H_3BTB (48.0 mg, 0.0816 mmol) was added to the clear solution and ultrasound for about

Please cite this article in press as: Chen et al., Boosting Highly Ordered Porosity in Lanthanum Metal-Organic Frameworks for Ring-Opening Polymerization of γ-Butyrolactone, Chem (2020), https://doi.org/10.1016/j.chempr.2020.11.019

1 min. The flask was tightly capped and heated in an oven at 85°C under static conditions. After 24 h, the colorless bulk crystals were obtained. The sample was washed with DMF and methanol each for 3 times. After drying at 150°C under vacuum for 12 h, La-BTB was obtained a as comparison.

Syntheses of NNU-mIM-x with the Addition of 1-Methylimidazole

$La(NO_3)_3 \cdot 6H_2O$ (138.6 mg, 0.320 mmol) was dissolved in 16 mL DMF/MeOH/H_2O (6:6:1) mixed solution with ultrasound for about 5 min in a 20 mL flask. H_3BTB (48.0 mg, 0.0816 mmol) was added to the clear solution and ultrasound for about 1 min. Different amounts of 1-mIM (from 0.4 to 3.6 mL) was added to the mixed solution and ultrasound for about 10 min. The flask was tightly capped and heated in an oven at 85°C under static conditions. After 24 h, the product was obtained. The sample was washed with DMF and methanol each for 3 times. After drying at 150°C under vacuum for 12 h, **NNU-mIM-x** (x, stands for the amount of 1-mIM added for every 0.4 mL) was obtained. La-BTB is equivalent to **NNU-mIM-0**.

Chemical Stability Tests

Chemical stability tests were performed through immersing the sample in various organic chemicals (e.g., aniline, n-hexane, tetrahydrofuran [THF], and chloroform) for 3 days, aqueous HCl solution (pH = 1), aqueous NaOH solution (pH = 12) for 24 h, water (RT) for 10 days and boiling water (100°C) for 3 days. All the samples after tests were collected by centrifugation and dried for further characterization.

Thermal Stability Tests

The thermal stability tests in air or N_2 were conducted by heating the sample from RT to target temperatures with a 10°C min^{-1} heating rate in a pipe furnace and kept at target temperatures for 30 min. After heat treatment, the sample was collected and characterized by PXRD tests.

NH_3-TPD Tests

NH_3-TPD test was conducted by the pulse technique using a Micromeritics AutoChem II 2920 instrument using thermal conductivity detector (TCD) detection. Before NH_3-TPD test, the sample was outgassed at 180°C for 24 h. During the NH_3-TPD test, the sample (~50 mg) was pretreated under the flow of helium (30 mL min^{-1}) at 300°C for 3 h to remove water. Then the temperature was lowered to RT under the flow of helium. The ammonia sorption was performed at 100°C for about 20 min. The NH_3-TPD data were collected from 50°C to 500°C under a heating rate of 10°C min^{-1} under the flow of helium and analyzed by gas chromatography (GC) spectra. The amount of ammonia was further analyzed to reflect the defects and acid amount of **NNU-mIM-x** (x = 1, 2, 3, 4, and 5).

Catalysis Experiments of La-BTB and NNU-mIM-x (x = 1, 2, 3, 4, and 5)

γ-BL (421.8 mg, 5 mmol) and Ph_2CHOH (100.0 mg, 0.5 mmol) was dissolved in 0.115 mL THF. catalyst (La-BTB or **NNU-mIM-x**, 100.0 mg, ~0.3 mmol) was added into the solution under vigorous stirring. The reaction was carried out under atmospheric pressure with magnetic stirring for the appropriate time (24 h) at -40°C. After the reaction was complete, the mixture was quenched by the addition of HCl (5%, 5 mL) acidified methanol. The quenched mixture was precipitated into cold methanol (100 mL), filtered, washed with methanol to remove any unreacted monomer, and dried in a vacuum oven at room temperature to a constant weight. Then the precipitated polymer was re-dissolved in THF to remove the precipitated catalyst. Finally, the product was obtained through evaporating the solvent of THF. All the catalysis experiments are conducted in triplicate to give the average data.

Please cite this article in press as: Chen et al., Boosting Highly Ordered Porosity in Lanthanum Metal-Organic Frameworks for Ring-Opening Polymerization of γ-Butyrolactone, Chem (2020), https://doi.org/10.1016/j.chempr.2020.11.019

For the recycle experiments, **NNU-mIM-3** was activated by Soxhlet extractor with CH_2Cl_2 as the solvent at 80°C (6 h for three times) after each cycle. After drying under vacuum (120°C for 12 h), the recovered sample was directly used for the next cycle.

For the catalysis experiments with the addition of various additives, **NNU-mIM-3** was selected as the catalyst. The catalysis procedures are conducted under similar conditions expect that various additives such as diethylamine, triethylamine, 1-methylimidazole, 1,10-phenanthroli, 5-bromosalicylic acid, or benzenesulfonic acid were added (the amount of additive was 20 μL). To determine the best condition of diethylamine, different amounts of diethylamine (i.e., 10, 20 and 30 μL) were tested under similar conditions. All the catalysis experiments were conducted in triplicate to give the average data.

Catalytic Performance of the Comparisons

γ-BL (421.8 mg, 5 mmol) and Ph_2CHOH (100.0 mg, 0.5 mmol) and comparisons (i.e., $La(NO_3)_3 \cdot 6H_2O$ [144.0 mg, 0.3 mmol] and H_3BTB [147.0 mg, 0.3 mmol]) were added into the reactor. The reactor was carried out under atmospheric pressure and was conducted with magnetic stirring for an appropriate time (24 h) at −40°C. After the reaction, the product treatment followed similar procedures as that of **NNU-mIM-x**. All the catalysis experiments were conducted in triplicate to give the average data.

Thermal Feedstock Recycling of PγBL

A sealed autoclave containing 100.0 mg purified PγBL was heated at 220°C for 1 h. After cooling to room temperature, the colorless liquid was formed and confirmed to be the recycled monomer γ-BL by ^{1}H NMR analysis.

The Catalysis Experiments of NNU-mIM-3 with β-BL and δ-VL

β-BL (430.5 mg, 5 mmol) or δ-VL (500.6 mg, 5 mmol), Ph_2CHOH (100.0 mg, 0.5 mmol) were dissolved in 0.115 mL THF. **NNU-mIM-3** (100.0 mg, ~0.3 mmol) was added into the solution under vigorous stirring. The reaction was carried out under normal pressure and room temperature with magnetic stirring for 16 h. After the reaction was completed, the mixtures were treated with similar procedures as that of γ-BL. All the catalysis experiments were conducted in triplicate to give the average data.

SUPPLEMENTAL INFORMATION

Supplemental Information can be found online at https://doi.org/10.1016/j.chempr.2020.11.019.

ACKNOWLEDGMENTS

This work was financially supported by NSFC (no. 21622104, 21701085, 21871125, 21871141, 21871142, and 21901122); the NSF of Jiangsu Province of China (no. BK20171032); the Natural Science Research of Jiangsu Higher Education Institutions of China (no. 17KJB150025 and 19KJB150011) and the project funded by China Postdoctoral Science Foundation (no. 2018M630572 and 2019M651873); Priority Academic Program Development of Jiangsu Higher Education Institutions; and the Foundation of Jiangsu Collaborative Innovation Center of Biomedical Functional Materials.

AUTHOR CONTRIBUTIONS

Y.-Q.L., Y.C., and Y.-J.C. conceived the idea. Y.-J.C., H.-J.Z., Y.Q., Y.C., S.-L.L., and Y.-Q.L. designed the experiments, collected and analyzed the data. X.H., Y.-J.C., Y.-R.W., H.-J.Z., R.-X.Y., and Y.-H.K assisted with the experiments and

characterizations. Y.C. and Y.-J.C. wrote the manuscript. All authors discussed the results and commented on the manuscript.

DECLARATION OF INTERESTS

The authors declare no competing interests.

Received: May 19, 2020
Revised: July 14, 2020
Accepted: November 16, 2020
Published: December 16, 2020

REFERENCES

1. Geyer, R., Jambeck, J.R., and Law, K.L. (2017). Production, use, and fate of all plastics ever made. Sci. Adv. *3*, e1700782.
2. Sardon, H., and Dove, A.P. (2018). Plastics recycling with a difference. Science *360*, 380–381.
3. Lebreton, L., Slat, B., Ferrari, F., Sainte-Rose, B., Aitken, J., Marthouse, R., Hajbane, S., Cunsolo, S., Schwarz, A., Levivier, A., et al. (2018). Evidence that the great pacific garbage patch is rapidly accumulating plastic. Sci. Rep. *8*, 4666.
4. Yoshida, S., Hiraga, K., Takehana, T., Taniguchi, I., Yamaji, H., Maeda, Y., Toyohara, K., Miyamoto, K., Kimura, Y., and Oda, K. (2016). A bacterium that degrades and assimilates poly(ethylene terephthalate). Science *351*, 1196–1199.
5. Hopewell, J., Dvorak, R., and Kosior, E. (2009). Plastics recycling: challenges and opportunities. Philos Trans. R. Soc. Lond. B Biol. Sci. *364*, 2115–2126.
6. Osborne, I.S. (2015). Designing mechanical complexity. Science *349*, 42.1–4242.
7. Zhang, X., Fevre, M., Jones, G.O., and Waymouth, R.M. (2018). Catalysis as an enabling science for sustainable polymers. Chem. Rev. *118*, 839–885.
8. Hillmyer, M.A., and Tolman, W.B. (2014). Aliphatic polyester block polymers: renewable, degradable, and sustainable. Acc. Chem. Res. *47*, 2390–2396.
9. Sarazin, Y., and Carpentier, J.F. (2015). Discrete cationic complexes for ring-opening polymerization catalysis of cyclic esters and epoxides. Chem. Rev. *115*, 3564–3614.
10. Bozell, J.J., and Petersen, G.R. (2010). Technology development for the production of biobased products from biorefinery carbohydrates—the US Department of Energy's "top 10" revisited. Green Chem. *12*, 539.
11. Martin, D.P., and Williams, S.F. (2003). Medical applications of poly-4-hydroxybutyrate: a strong flexible absorbable biomaterial. Biochem. Eng. J. *16*, 97–105.
12. Hu, D., Chung, A.L., Wu, L.P., Zhang, X., Wu, Q., Chen, J.C., and Chen, G.Q. (2011). Biosynthesis and characterization of polyhydroxyalkanoate block copolymer P3HB-b-P4HB. Biomacromolecules *12*, 3166–3173.
13. Saiyasombat, W., Molloy, R., Nicholson, T.M., Johnson, A.F., Ward, I.M., and Poshyachinda, S. (1998). Ring strain and polymerizability of cyclic esters. Polymer *39*, 5581–5585.
14. Houk, K.N., Jabbari, A., Hall, H.K., and Aleman, C. (2008). Why delta-valerolactone polymerizes and gamma-butyrolactone does not. J. Org. Chem. *73*, 2674–2678.
15. Moore, T., Adhikari, R., and Gunatillake, P. (2005). Chemosynthesis of bioresorbable poly(gamma-butyrolactone) by ring-opening polymerisation: a review. Biomaterials *26*, 3771–3782.
16. Yamashita, K., Yamamoto, K., and Kadokawa, J.I. (2014). Acid-catalyzed ring-opening polymerization of γ-butyrolactone under high-pressure conditions. Chem. Lett. *43*, 213–215.
17. Oish, Taguchi, A., Y., and Fujita, K. (2003). Japan Patent JP2003252968.
18. Oishi, A., Taguchi, Y., Fujita, K., Ikeda, Y., and Masuda, T. (2000). Japan Patent JP2000281767.
19. Hong, M., and Chen, E.Y. (2016). Completely recyclable biopolymers with linear and cyclic topologies via ring-opening polymerization of gamma-butyrolactone. Nat. Chem. *8*, 42–49.
20. Hong, M., and Chen, E.Y. (2016). Towards truly sustainable polymers: a metal-free recyclable polyester from biorenewable non-strained gamma-butyrolactone. Angew. Chem. Int. Ed. Engl. *55*, 4188–4193.
21. Zhao, N., Ren, C., Li, H., Li, Y., Liu, S., and Li, Z. (2017). Selective ring-opening polymerization of non-strained gamma-butyrolactone catalyzed by a cyclic trimeric phosphazene base. Angew. Chem. Int. Ed. Engl. *56*, 12987–12990.
22. Shen, Y., Zhao, Z., Li, Y., Liu, S., Liu, F., and Li, Z. (2019). A facile method to prepare high molecular weight bio-renewable poly(γ-butyrolactone) using a strong base/urea binary synergistic catalytic system. Polym. Chem. *10*, 1231–1237.
23. Shen, Y., Zhang, J., Zhao, Z., Zhao, N., Liu, F., and Li, Z. (2019). Preparation of amphiphilic poly(ethylene glycol)- b-poly(gamma-butyrolactone) diblock copolymer via ring opening polymerization catalyzed by a cyclic trimeric phosphazene base or alkali alkoxide. Biomacromolecules *20*, 141–148.
24. Shen, Y., Zhang, J., Zhao, N., Liu, F., and Li, Z. (2018). Preparation of biorenewable poly(γ-butyrolactone)-b-poly(l-lactide) diblock copolyesters via one-pot sequential metal-free ring-opening polymerization. Polym. Chem. *9*, 2936–2941.
25. Zhang, C.J., Hu, L.F., Wu, H.L., Cao, X.H., and Zhang, X.H. (2018). Dual organocatalysts for highly active and selective synthesis of linear poly(γ-butyrolactone)s with high molecular weights. Macromolecules *51*, 8705–8711.
26. Lin, L., Han, D., Qin, J., Wang, S., Xiao, M., Sun, L., and Meng, Y. (2018). Nonstrained γ-butyrolactone to high-molecular-weight poly(γ-butyrolactone): facile bulk polymerization using economical ureas/alkoxides. Macromolecules *51*, 9317–9322.
27. Walther, P., Frey, W., and Naumann, S. (2018). Polarized olefins as enabling (Co)catalysts for the polymerization of γ-butyrolactone. Polym. Chem. *9*, 3674–3683.
28. Sordakis, K., Tang, C., Vogt, L.K., Junge, H., Dyson, P.J., Beller, M., and Laurenczy, G. (2018). Homogeneous catalysis for sustainable hydrogen storage in formic acid and alcohols. Chem. Rev. *118*, 372–433.
29. Li, H., Eddaoudi, M., O'Keeffe, M., and Yaghi, O.M. (1999). Design and synthesis of an exceptionally stable and highly porous metal-organic framework. Nature *402*, 276–279.
30. Kitaura, R., Kitagawa, S., Kubota, Y., Kobayashi, T.C., Kindo, K., Mita, Y., Matsuo, A., Kobayashi, M., Chang, H.-C., Ozawa, T.C., et al. (2002). Formation of a one-dimensional array of oxygen in a microporous metal-organic solid. Science *298*, 2358–2361.
31. Shekhah, O., Belmabkhout, Y., Chen, Z., Guillerm, V., Cairns, A., Adil, K., and Eddaoudi, M. (2014). Made-to-order metal-organic frameworks for trace carbon dioxide removal and air capture. Nat. Commun. *5*, 4228.
32. Yuan, S., Feng, L., Wang, K., Pang, J., Bosch, M., Lollar, C., Sun, Y., Qin, J., Yang, X., Zhang, P., et al. (2018). Stable metal-organic frameworks: design, synthesis, and applications. Adv. Mater. *30*, e1704303.
33. Liu, L., and Corma, A. (2018). Metal catalysts for heterogeneous catalysis: from single atoms to nanoclusters and nanoparticles. Chem. Rev. *118*, 4981–5079.
34. She, Z.W., Kibsgaard, J., Dickens, C.F., Chorkendorff, I., Norskov, J.K., and Jaramillo, T.F. (2017). Combining theory and experiment

in electrocatalysis: insights into materials design. Science *355*, eaad4998.

35. Molnár, Á., and Papp, A. (2017). Catalyst recycling—a survey of recent progress and current status. Coord. Chem. Rev. *349*, 1–65.

36. Duan, J., Higuchi, M., Horike, S., Foo, M.L., Rao, K.P., Inubushi, Y., Fukushima, T., and Kitagawa, S. (2013). High CO2/CH4 and C2 Hydrocarbons/CH4 selectivity in a chemically robust porous coordination polymer. Adv. Funct. Mater. *23*, 3525–3530.

37. Lixin, Z., Bo, W., Shiyan, Y., and Daosen, J. (1993). XPS study of metal complexes with an unsymmetrical tridentate Schiff base. Polyhedron *12*, 1607–1611.

38. Jiang, H., Wang, Q., Wang, H., Chen, Y., and Zhang, M. (2016). MOF-74 as an efficient catalyst for the low-temperature selective catalytic reduction of NOx with NH3. ACS Appl. Mater. Interfaces *8*, 26817–26826.

39. Pan, Y., Yuan, B., Li, Y., and He, D. (2010). Multifunctional catalysis by Pd@MIL-101: one-step synthesis of methyl isobutyl ketone over palladium nanoparticles deposited on a metal-organic framework. Chem. Commun.(Camb). *46*, 2280–2282.

40. Jiang, J., and Yaghi, O.M. (2015). Brønsted acidity in metal–organic frameworks. Chem. Rev. *115*, 6966–6997.

41. Li, Q., Jiang, S., Ji, S., Shi, D., and Li, H. (2015). Synthesis of magnetically recyclable MOF-5@SiO2@Fe3O4 catalysts and their catalytic performance of Friedel–crafts alkylation. J. Porous Mater. *22*, 1205–1214.

42. Penczek, S., Duda, A., Kaluzynski, K., Lapienis, G., Nyk, A., and Szymanski, R. (1993). Thermodynamics and kinetics of ring-opening polymerization of cyclic alkylene phosphates. Makromol. Chem. Macromol. Symp. *73*, 91–101.

43. Li, P.Z., Wang, X.J., Liu, J., Lim, J.S., Zou, R., and Zhao, Y. (2016). A triazole-containing metal-organic framework as a highly effective and substrate size-dependent catalyst for CO2 conversion. J. Am. Chem. Soc. *138*, 2142–2145.

44. Ji, G., Yang, Z., Zhang, H., Zhao, Y., Yu, B., Ma, Z., and Liu, Z. (2016). Hierarchically mesoporous o-hydroxyazobenzene polymers: synthesis and their applications in CO2 capture and conversion. Angew. Chem. Int. Ed. Engl. *55*, 9685–9689.

45. Xu, C., Yu, I., and Mehrkhodavandi, P. (2012). Highly controlled immortal polymerization of β-butyrolactone by a dinuclear indium catalyst. Chem. Commun. *48*, 6806–6808.

46. Kan, S., Jin, Y., He, X., Chen, J., Wu, H., Ouyang, P., Guo, K., and Li, Z. (2013). Imidodiphosphoric acid as a bifunctional catalyst for the controlled ring-opening polymerization of δ-valerolactone and ε-caprolactone. Polym. Chem. *4*, 5432–5439.